## NEUROIMMUNOLOGY

# Choline acetyltransferase–expressing T cells are required to control chronic viral infection

Maureen A. Cox[1], Gordon S. Duncan[1], Gloria H. Y. Lin[1]*, Benjamin E. Steinberg[1,2]†, Lisa X. Yu[3], Dirk Brenner[1,4,5], Luke N. Buckler[1], Andrew J. Elia[1], Andrew C. Wakeham[1], Brian Nieman[3,6], Carmen Dominguez-Brauer[1], Alisha R. Elford[1], Kyle T. Gill[1], Shawn P. Kubli[1], Jillian Haight[1], Thorsten Berger[1], Pamela S. Ohashi[1,7], Kevin J. Tracey[8], Peder S. Olofsson[8,9], Tak W. Mak[1,6,7,10]‡

Although widely studied as a neurotransmitter, T cell–derived acetylcholine (ACh) has recently been reported to play an important role in regulating immunity. However, the role of lymphocyte-derived ACh in viral infection is unknown. Here, we show that the enzyme choline acetyltransferase (ChAT), which catalyzes the rate-limiting step of ACh production, is robustly induced in both CD4+ and CD8+ T cells during lymphocytic choriomeningitis virus (LCMV) infection in an IL-21–dependent manner. Deletion of *Chat* within the T cell compartment in mice ablated vasodilation in response to infection, impaired the migration of antiviral T cells into infected tissues, and ultimately compromised the control of chronic LCMV clone 13 infection. Our results reveal a genetic proof of function for ChAT in T cells during viral infection and identify a pathway of T cell migration that sustains antiviral immunity.

T he prototypic neurotransmitter acetylcholine (ACh) was the first neurotransmitter identified (1, 2). ACh has numerous physiological roles, including mediating skeletal and smooth muscle contraction, communication between neurons, and induction of vasodilation (1–3). In addition to neurons, a population of CD4+ T cells and B cells express the enzyme choline acetyltransferase (ChAT) (4, 5), which catalyzes the rate-limiting step of ACh production. Although these ChAT-expressing T cells have a demonstrated impact on blood pressure (6) and the release of inflammatory cytokines (4), the biological role of immune-derived ACh during infection has not been elucidated. In this study, we have determined

that *Chat* is induced by IL-21 in T cells during infection to facilitate T cell entry into infected tissues, thereby genetically identifying the function of T cell–derived ACh during an immune response.

*Chat*+ CD4+ T cells uniformly exhibit an "antigen-experienced" phenotype (4). Yet, the signals that drive *Chat* expression in T cells are undefined. We infected *Chat*–green fluorescent protein (GFP) reporter mice (7) with the rapidly cleared Armstrong strain of lymphocytic choriomeningitis virus (LCMV-Arm). There was a massive increase in *Chat*-GFP expression in both CD4+ and CD8+ T cells 8 days postinfection (Fig. 1A). In splenic virus-specific T cells, expression rapidly declined after LCMV-Arm clearance (Fig. 1B), yet *Chat*-GFP expression was retained in both virus-specific CD4+ and CD8+ T cells from mice chronically infected with LCMV clone 13 (LCMV-Cl13) (Fig. 1B). GFP expression correlated with *Chat* mRNA in T cells (Fig. 1C). In CD4+ T cells, *Chat*-GFP was expressed by all subsets; however, expression was highest in T follicular helper (TFH) cells (fig. S1, A to D). In CD8+ T cells, there was no correlation with either memory precursor or short-lived effector phenotypes (fig. S1E). Furthermore, *Chat*-GFP was induced in germinal center (GC) B cells in the spleen, although *Chat* expression was not retained in this population during persistent infection (fig. S1, F and G). *Chat*-GFP was also induced in both CD4+ and CD8+ T cells after vesicular stomatitis virus infection (fig. S1H).

The kinetics of *Chat*-GFP expression during acute and chronic infection implicates viral signals in driving *Chat* induction in T cells. Viral infection induces numerous cytokines that influence T cells, including type I interfer-

ons (IFN-I), interleukin-2 (IL-2), IL-6, IL-7, IL-10, IL-15, and IL-21 (8). We activated *Chat*-GFP P14 T cell receptor (TCR) transgenic T cells in vitro with the GP33 peptide in the presence or absence of these cytokines. The only condition that resulted in *Chat* induction in P14 cells in vitro was IL-21 with peptide stimulation (Fig. 1D and fig. S2A). We evaluated the contribution of IL-21 signaling to *Chat* induction in vivo by infecting IL-21 receptor–deficient (*Il21r*−/−) mice (9) expressing the *Chat*-GFP reporter with LCMV-Cl13. We observed a decrease in the fraction of both CD4+ and CD8+ T cells expressing *Chat*-GFP in *Il21r*−/− mice (Fig. 1E). Mice heterozygous for *Il21r* (*Il21r*+/−) showed a mixed phenotype. The expression of *Chat*-GFP in B cell populations was not reduced in *Il21r*−/− animals (Fig. 1E). *Chat*-GFP+ cells in *Il21r*−/− mice also demonstrated a lower mean fluorescence intensity (MFI) for the reporter molecule, suggesting reduced expression (Fig. 1F and fig. S2B).

IL-21 is critical for antiviral immunity (10–12). Thus, we investigated the role of IL-21–induced *Chat* in T cells (T-*Chat*) by using *Chat*flox mice (13) crossed with CD4-cre mice (14) to generate *Chat*flox/flox CD4-cre− (*Chat*WT) and *Chat*flox/flox CD4-cre+ (T-*Chat*KO) animals. Cre-driven recombination occurs at the double-positive stage in the thymus (14), resulting in deletion of *Chat* in both CD4+ and CD8+ T cells (fig. S3A) and a subsequent failure to produce ACh (fig. S3B). Notably, the loss of *Chat* specifically within T cells resulted in a failure to control LCMV-Cl13 in a subset of the animals (Fig. 2A), revealing that *Chat* expression in T cells is required during chronic infection. This failure to control LCMV-Cl13 corresponded to the attrition of virus-specific CD8+ T cells over time (Fig. 2B), poor cytokine production (Fig. 2C), and increased expression of inhibitory receptors (Fig. 2, D and E). There was no difference in the number of antiviral T cells in LCMV-Arm–infected T-*Chat*KO mice (fig. S4), which has also been reported for *Il21*−/− animals (15). Although we observed high *Chat* expression in TFH and GC B cells (fig. S1), there were no deficits in either antiviral CD4+ T cell numbers or in the anti-LCMV antibody response in T-*Chat*KO mice (fig. S5).

Loss of IL-21 signaling results in decreased T cell infiltration of tissues in bone marrow chimeras (16, 17). Thus, we evaluated tissue infiltration by *Il21r*−/− T cells during LCMV-Cl13 infection using intravascular staining (18). We found a reduction in virus-specific T cells that had migrated into infected livers of *Il21r*−/− mice (Fig. 3A). *Chat*-expressing T cells reduce blood pressure by producing ACh (3, 6), which may facilitate T cell entry into tissues by slowing blood flow. Consequently, we also found a reduction in virus-specific CD8+ T cells in both the liver and salivary gland of T-*Chat*KO mice after LCMV-Cl13 infection (Fig. 3, B and C). No difference in the number of circulating virus-specific cells was found in either *Il21r*−/− or T-*Chat*KO mice (fig. S6, A to C). We observed a similar trend in the liver for virus-specific CD4+ T cells (fig. S6D). Poor migration into tissues

[1]The Campbell Family Institute for Breast Cancer Research, Princess Margaret Cancer Centre, University Health Network, Toronto, ON M5G 2M9, Canada. [2]Department of Anesthesia, University of Toronto, Toronto, ON M5G 1E2, Canada. [3]Mouse Imaging Centre, The Hospital for Sick Children, Toronto, ON M5T 3H7, Canada. [4]Department of Infection and Immunity, Luxembourg Institute of Health, L-4354 Esch-sur-Alzette, Luxembourg. [5]Odense Research Center for Anaphylaxis (ORCA), Department of Dermatology and Allergy Center, Odense University Hospital, University of Southern Denmark, Odense, Denmark. [6]Ontario Institute for Cancer Research and Department of Medical Biophysics, University of Toronto, Toronto, ON M5G 2C1, Canada. [7]Department of Immunology, University of Toronto, Toronto, ON M5G 2C1, Canada. [8]Laboratory of Biomedical Science, Feinstein Institute for Medical Research, Manhasset, NY 11030, USA. [9]Center for Bioelectronic Medicine, Department of Medicine, Solna, Karolinska Institutet, Karolinska University Hospital, 17176 Stockholm, Sweden. [10]Department of Pathology, University of Hong Kong, Hong Kong.
*Present address: Trillium Therapeutics Inc., Mississauga, ON L5L 1J9, Canada. †Present address: Department of Anesthesia and Pain Medicine, The Hospital for Sick Children, Toronto, ON M5G 1X8, Canada.
‡Corresponding author. Email: tmak@uhnresearch.ca

**Fig. 1. *Chat* is induced in virus-specific T cells in an IL-21–dependent manner.** (**A**) *Chat*-GFP$^+$ and *Chat*-GFP$^-$ animals were infected with LCMV-Arm, and the expression of *Chat*-GFP in total CD4$^+$ (top) or CD8$^+$ (bottom) T cells 8 days postinfection was compared with expression in uninfected *Chat*-GFP$^+$ cohorts. Mean ± SEM, representative of two to four experimental cohorts, $n = 8$ to 12 mice for *Chat*-GFP$^+$, $n = 4$ for *Chat*-GFP$^-$. (**B**) The fraction of virus-specific CD4$^+$ (left) or CD8$^+$ (right) T cells expressing *Chat*-GFP was determined 8, 20, and 30 days post-infection with LCMV-Arm or LCMV-Cl13 by evaluating tetramer staining and *Chat*-GFP expression by flow cytometry. Composite data of two (Arm) or four (Cl13) experiments. $n = 7$ to 12 (Arm) and $n = 10$ to 27 (Cl13) animals per group per time point.



(**C**) Pooled splenocytes from $n = 5$ *Chat*-GFP mice infected 8 days previously with LCMV-Cl13 were sorted to obtain CD4$^+$ GFP$^+$, CD4$^+$ GFP$^-$, CD8$^+$ GFP$^+$, and CD8$^+$ GFP$^-$ populations. RNA was isolated from the cells, and expression of *Chat* and *Rsp9* was evaluated by reverse transcription polymerase chain reaction in technical triplicates. *Chat* expression in CD4$^+$ and CD8$^+$ populations was normalized to the expression in the relevant sorted GFP$^-$ population. Mean ± SEM, representative of two experimental cohorts. Ct, cycle threshold. (**D**) *Chat*-GFP$^+$ and *Chat*-GFP$^-$ P14 CD8$^+$ T cells were stimulated in vitro with GP33 peptide and indicated cytokines for 5 days. The expression of *Chat*-GFP in the P14 cells was determined by flow cytometry. Composite of two experimental cohorts, box plots indicate 25th to 75th percentile, line at median. Whiskers represent range minimum to maximum, $n = 5$ *Chat*-GFP$^+$ P14 mice. Significance tested using one-way analysis of variance (ANOVA), $P < 0.0001$, significance between samples determined by $t$ test (depicted). (**E**) *Il21r*$^{+/+}$ (dark gray), *Il21r*$^{+/-}$ (light gray), and *Il21r*$^{-/-}$ (white) mice expressing *Chat*-GFP were infected with LCMV-Cl13, and *Chat* expression was determined in splenocyte fractions 8 days post-infection by flow cytometry. Box and whiskers drawn with the Tukey method, line at median. Values outside of 1.5 times the interquartile range are depicted as individual symbols. Two-way ANOVA was performed ($P < 0.0001$), followed by multiple comparisons between groups. (**F**) Representative flow plots of virus-specific D$^b$(GP33)$^+$ (left) or D$^b$(GP276)$^+$ (right) CD8$^+$ T cells 8 days post-infection in *Il-21r*$^{+/+}$ or *Il-21r*$^{-/-}$ mice. Representative of two to three experimental cohorts, $n = 8$ to 13. Statistical significance determined by unpaired two-tailed $t$ test; $*P < 0.05$, $**P < 0.01$, $***P < 0.001$, $****P < 0.0001$.

could affect viral control, as fewer migrated cytotoxic T lymphocytes (CTLs) would result in the poor elimination of infected cells. In vivo CTL activity in the liver was impaired for two epitopes examined 8 days postinfection in T-*Chat*$^{KO}$ mice (Fig. 3D), despite equivalent expression of granzyme B and degranulation (Fig.
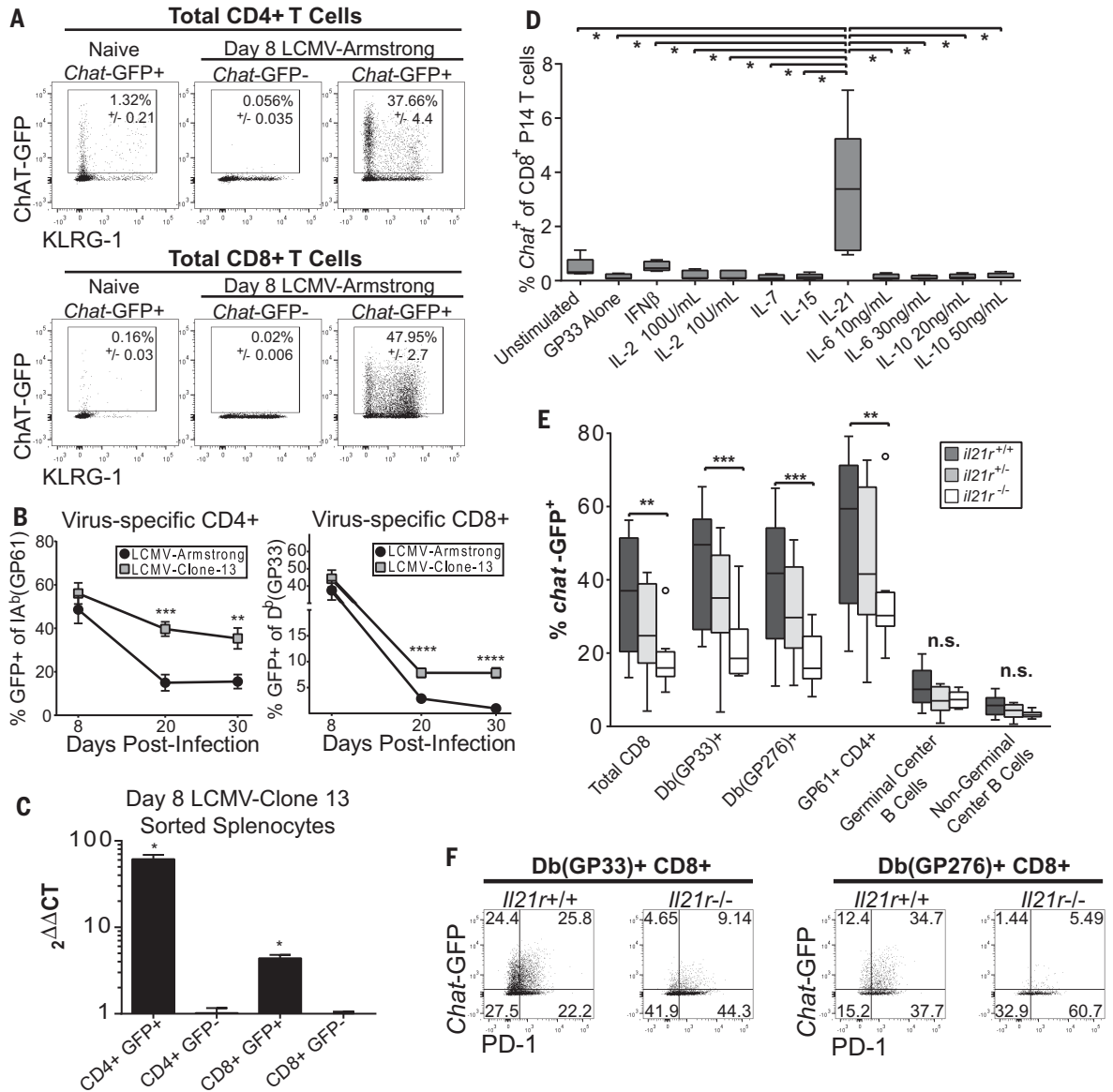
3E) by noncirculating CTLs. Furthermore, this diminution in CTL activity was observed only for the GP33 epitope in the spleen (Fig. 3D), suggesting that the poor CTL activity in the liver was not due to intrinsic defects in the cells but rather their impaired infiltration of tissues.

We tested whether *Chat* expression in T cells functions in a cell-intrinsic manner by transplanting *Chat*$^{WT}$ or T-*Chat*$^{KO}$ TCR transgenic P14 T cells into congenic recipient *Chat*$^{WT}$ or T-*Chat*$^{KO}$ mice and infecting them with LCMV-Cl13. We then quantified migration capacity of the P14 cells (Fig. 3F). Briefly, we examined the

**Fig. 2. Loss of *Chat* in T cells compromises control of viral infection.** (**A**) *Chat*[WT] and T-*Chat*[KO] were infected with LCMV-Cl13. Viral titers in the serum of either *Chat*[WT] (black) or T-*Chat*[KO] (white) were determined at indicated time points by plaque assay. Each symbol indicates an individual animal. Composite data of two to three experimental replicates, *n* = 11 to 23. Line at limit of detection, 333 PFU/ml (PFU, plaque-forming units). (**B**) The number of D$^b$(GP33)$^+$ or D$^b$(GP276)$^+$ CD8$^+$ splenocytes was determined over time by tetramer staining. Mean ± SEM, composite of three to four experimental cohorts, *n* = 10 to 16. (**C**) Splenocytes from *Chat*[WT] and T-*Chat*[KO] animals were stimulated with the GP276 peptide in vitro, and the number of cells



producing IFN-γ, tumor necrosis factor–α (TNF-α), and IL-2 was quantified by intracellular cytokine staining. The fraction of the total D$^b$(GP276)-specific cells which are nonfunctional was determined by comparing the number of cytokine-producing cells to the number of tetramer-binding cells. Of the functional cells, the fraction which are monofunctional or polyfunctional was determined. Mean of two to three experimental cohorts, *n* = 9 (day 30), *n* = 8 (day 60). (**D**) Representative flow plot of PD-1, Tim3, and LAG-3 expression in virus-specific CD8$^+$ T cells 60 days postinfection in *Chat*[WT] (black) or T-*Chat*[KO] (gray) mice. (**E**) MFI for PD-1, Tim3, and LAG-3 in virus-specific CD8$^+$ T cells 60 days postinfection in *Chat*[WT] (black) or T-*Chat*[KO] (white) mice. Mean ± SEM, composite of three experimental cohorts, *n* = 13 to 15. Statistical significance for all samples determined by unpaired two-tailed *t* test; *P < 0.05, **P < 0.01, ***P < 0.001.

total noncirculating D$^b$(GP33)$^+$ in the spleen and organs and determined what percentage of these D$^b$(GP33)$^+$ cells were donor P14 cells. This percentage in each organ was then compared against the percentage in the spleen of that individual animal to determine whether the P14 cells had migrated in a superior (ratio > 1), inferior (ratio < 1), or equivalent (ratio = 1) manner compared with the endogenous D$^b$(GP33)$^+$ T cells (Fig. 3F). In control mice (WT P14→WT recipients and KO P14→KO recipients), the frequency of P14 cells was similar in the spleen and organs, resulting in a ratio of ~1 (Fig. 3G and fig. S6G). However, in T-*Chat*[KO] mice receiving *Chat*[WT] P14 cells, we observed a greater frequency of *Chat*[WT] P14 cells in the liver and kidney than would be predicted by their rate of occurence in

the spleen (Fig. 3G and fig. S6G). Thus, *Chat*[WT] cells were more efficient at seeding these peripheral organs than T-*Chat*[KO] cells in the same animal. When T-*Chat*[KO] P14 cells were transplanted into a *Chat*[WT] recipient, they migrated just as well as endogenous *Chat*[WT] cells, indicating that the observed differences were not due to an intrinsic failure of T-*Chat*[KO] cells to adhere or sense chemokines. We postulated that this migratory advantage of *Chat*[WT] cells in a T-*Chat*[KO] host was due to local changes in the vasculature induced by the presence of *Chat*$^+$ T cells and would still be present in *Chat*[WT] recipients of T-*Chat*[KO] P14 cells.

Vasodilation is critical for immune responses and is one of the hallmarks of inflammation facilitating the entry of immune cells into infected tissues. Not only do *Il21r*$^{-/-}$ mice exhibit

smaller arterial connections in the brain (*19*), T-*Chat*[KO] mice exhibit higher blood pressure than *Chat*[WT] littermates (*6*), indicating that they also have smaller arteries. ACh signaling has long been known to induce vasodilation (*20*). We posited that *Chat*$^+$ T cells induced by infection are the primary mediators of vasodilation via the release of ACh and that loss of *Chat* in T cells would consequently abrogate infection-driven vasodilation. Upon imaging the liver arterial vasculature of naïve and LCMV-Cl13–infected *Chat*[WT] and T-*Chat*[KO] mice (movies S1 to S4), we found that infection-induced vasodilation in the liver was completely abrogated in T-*Chat*[KO] mice, in contrast to their *Chat*[WT] counterparts (Fig. 4, A and B), resulting in fewer detectable terminal branches (fig. S7A)
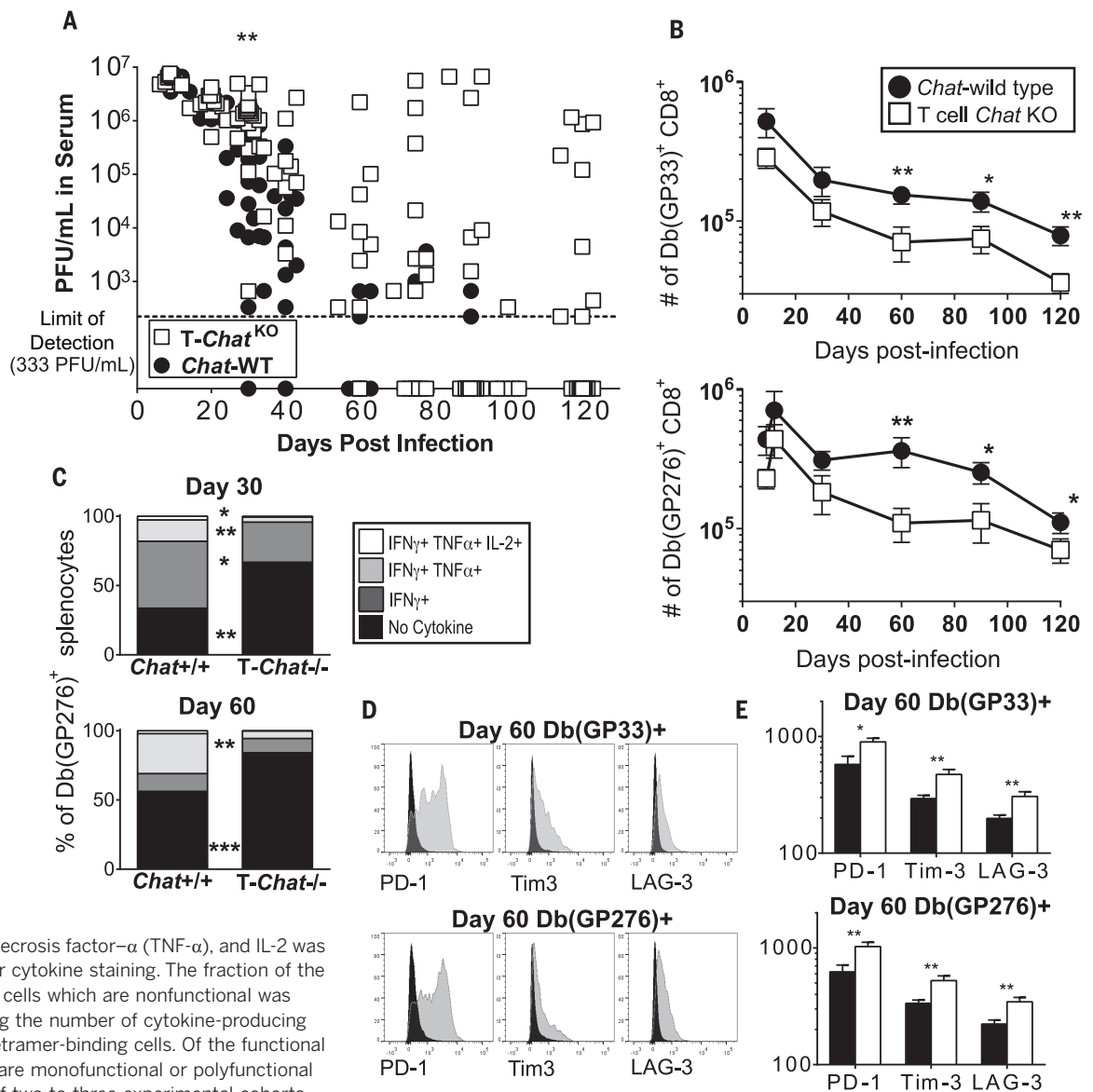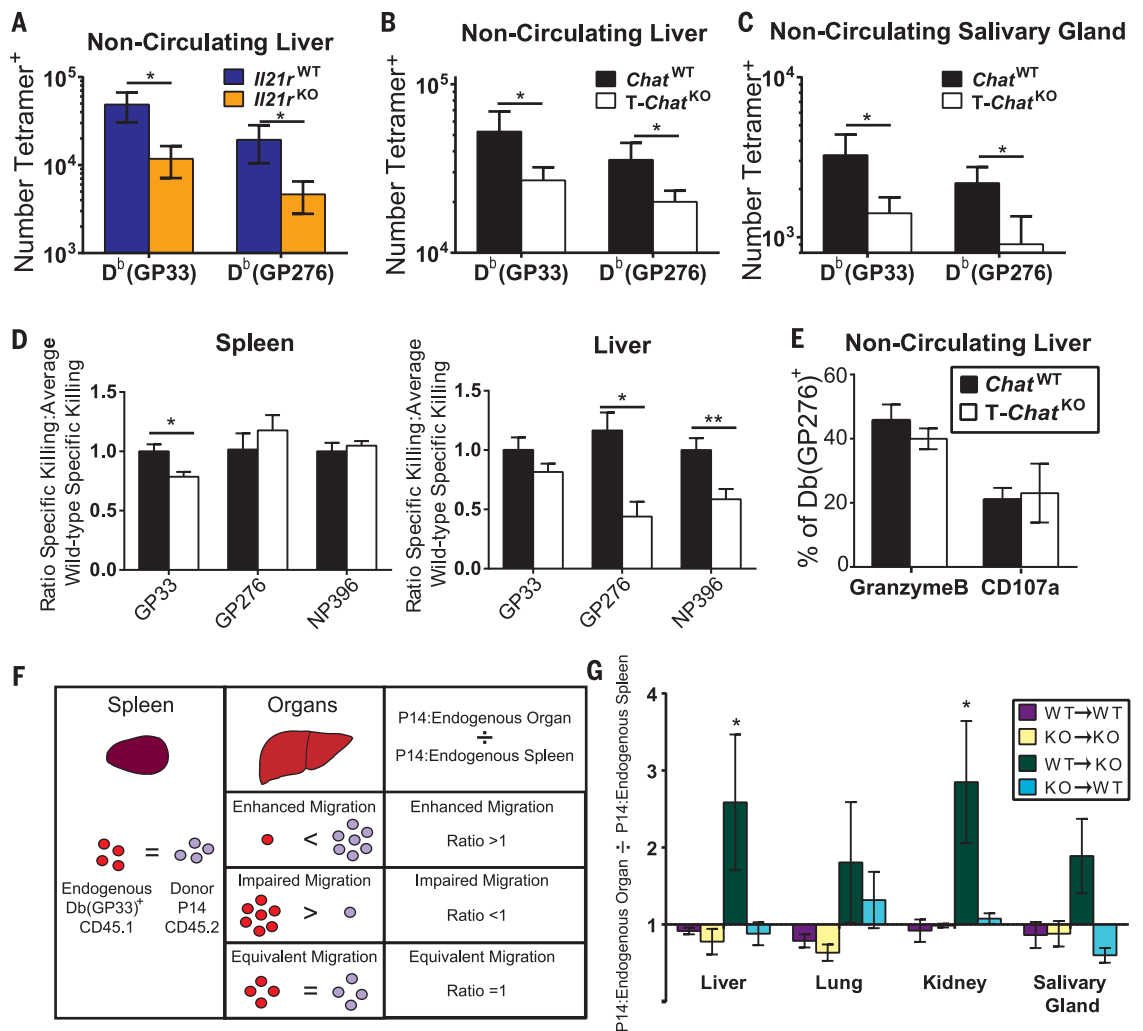
**Fig. 3. IL-21–driven *Chat* expression in T cells facilitates migration into infected tissues.** (**A**) Day 8 LCMV-Cl13 infected *Il21r*$^{+/+}$ (blue) or *Il21r*$^{-/-}$ (orange) animals were injected intravenously with α-CD8-FITC (FITC, fluorescein isothiocyanate) 3 min before being euthanized. Livers were then processed, washed, and stained for CD8, tetramer, and inhibitory receptors. FITC$^-$ liver-infiltrating CD8$^+$ T cells were enumerated. Composite of three experimental cohorts, *n* = 10 to 11. (**B** and **C**) The number of virus-specific CD8 T cells in the tissue of *Chat*$^{WT}$ (black) and T-*Chat*$^{KO}$ (white) mice was determined in liver (B) and salivary gland (C) by intravascular staining as in (A). Mean + SEM, composite of five experimental cohorts for liver, two experimental cohorts for salivary gland, *n* = 12 to 22. (**D**) In vivo cytolytic activity was determined in the spleen and liver of *Chat*$^{WT}$ or T-*Chat*$^{KO}$ mice 8 days post–LCMV-Cl13 infection. Mean + SEM, composite of three to four experimental cohorts, *n* = 15 (GP276 and NP396), *n* = 23 (GP33). (**E**) The fraction of liver-infiltrating D$^b$(GP276)-specific CD8 T cells expressing granzyme B was determined by intravascular staining as in (A). The fraction of liver-infiltrating CD8 T cells expressing CD107a and IFN-γ after in vitro stimulation with GP276 was compared with the total number of liver-infiltrating D$^b$(GP276)$^+$ cells to determine the percent of GP276-specific cells capable of degranulation. Mean ± SEM, composite of two experimental cohorts, *n* = 11 to 12. (**F**) Analysis schematic for P14 transfer experiments. *Chat*$^{WT}$ P14 or *Chat*$^{KO}$ P14 T cells were transferred into either *Chat*$^{WT}$ or T-*Chat*$^{KO}$ recipient mice, which were subsequently infected with LCMV-Cl13. Intravascular cells in different tissues were marked as in (A), 30 days postinfection. The D$^b$(GP33)-specific nonvascular cells were evaluated to determine the relative ratio of endogenous and P14 cells in the spleen and peripheral organs. The relative abundance of P14 cells in the organs was then compared with that in the spleen to determine whether P14 cells migrated better than, as well as, or worse than the endogenous D$^b$(GP33)-specific cells. (**G**) The ratio of migrated P14 cells to endogenous D$^b$(GP33)$^+$ cells was determined as described in (F). Mean ± SEM, composite of two experimental cohorts for controls and four experimental cohorts, *n* = 5 to 10 control animals, *n* = 12 to 17 experimental animals. Statistical significance for all samples determined by unpaired two-tailed *t* test; *$P < 0.05$, **$P < 0.01$, ***$P < 0.001$, ****$P < 0.0001$.

and smaller mean vessel diameter at equivalent branch depths (fig. S7B).

The blood vessel phenotype in T-*Chat*$^{KO}$ mice was reversed with short-term treatment with the vasodilator minoxidil (Fig. 4C, fig. S7, and movie S5). Thus, these differences were not developmental but reflective of poor vasodilation in the absence of T-*Chat*. Furthermore, treatment of wild-type mice with the vasoconstrictor L-NAME was sufficient to recapitulate the vascular phenotype observed in T-*Chat*$^{KO}$ mice (Fig. 4C, fig. S7, and movie S6). Minoxidil treatment was sufficient to restore viral control in T-*Chat*$^{KO}$ mice and also augmented viral con-

trol in *Chat*$^{WT}$ animals (Fig. 4D). Moreover, viral titers were significantly higher in wild-type mice treated with L-NAME on days 6 through 12 postinfection when compared with phosphate-buffered saline (PBS)–treated controls (Fig. 4E). Thus, vasodilation mediated by *Chat*-expressing T cells is critical for appropriate viral control.

IL-21 supports antiviral immunity beyond *Chat* induction and vasomodulation (*21*). Indeed, treatment with minoxidil was not sufficient to fully rescue *Il21r*$^{-/-}$ mice, although this treatment did reduce viral titers compared with vehicle-treated *Il21r*$^{-/-}$ mice (Fig. 4F). Efficient migration of effector T cells into tissues is crit-

ical for the control of viral infections (*22*) and is also of great interest for immunotherapy directed at tumors (*23*). In addition to its other reported roles during infection, IL-21 signaling enhances the efficacy of expanded tumor-infiltrating lymphocytes to combat cancer (*24, 25*). Here, we report that IL-21, a cytokine critical for control of chronic infection (*10–12*), drives the expression of *Chat* in T cells to facilitate their migration into infected tissues. These findings underscore the role for IL-21 during the host response to infection and establish a cholinergic mechanism for regulating cellular migration into tissues.
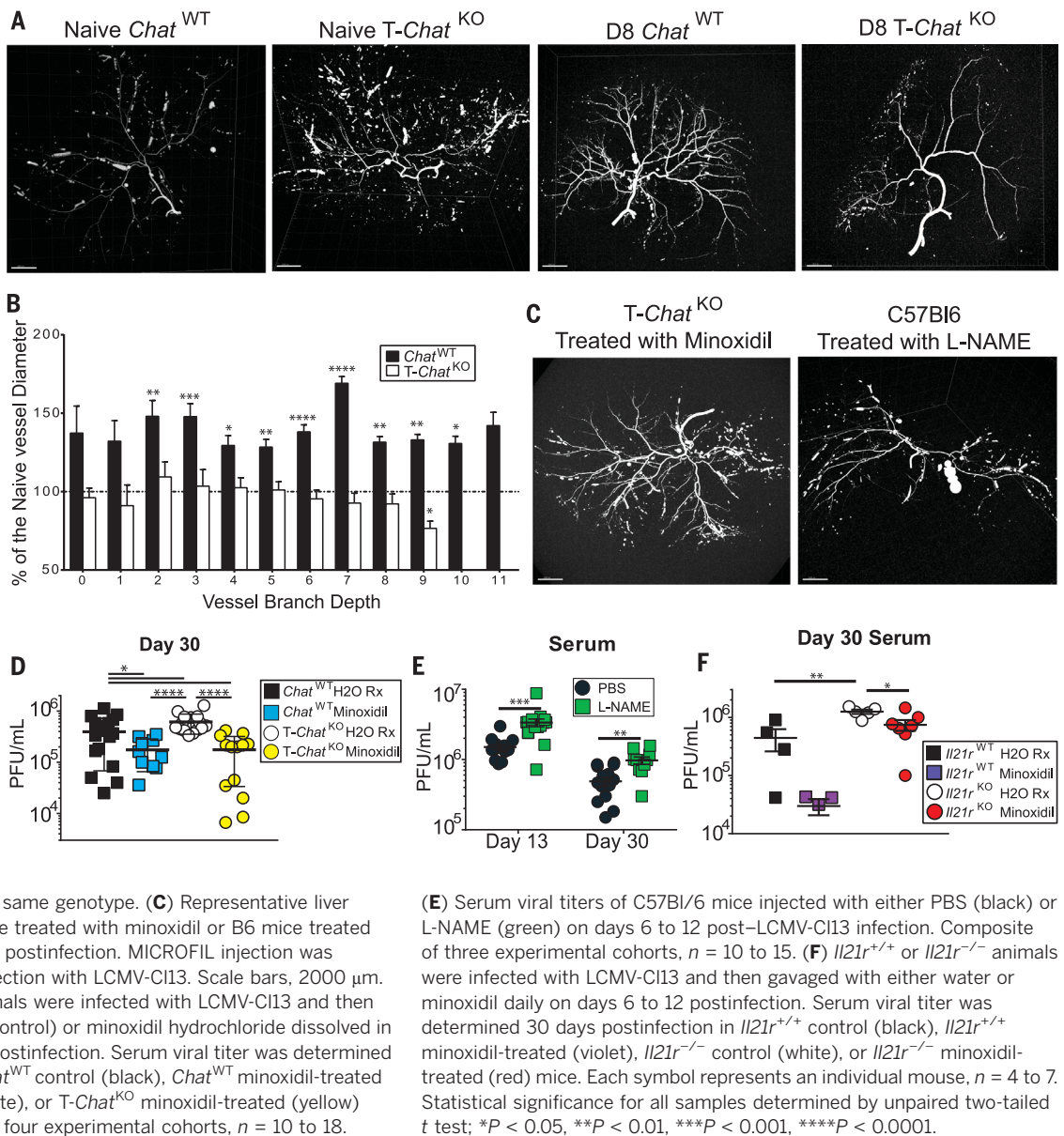
**Fig. 4. Vasodilation during infection is dependent on *Chat*-expressing T cells and is critical for viral control.**



(**A**) Representative liver arterial tree of naïve (left) or day 8 post–LCMV-Cl13 infection (right) *Chat*[WT] and T-*Chat*[KO] mice imaged using MICROFIL and micro–computed tomography scan. Representative of two (naïve) or four (day 8) mice. Scale bars, 2000 μm. (**B**) Mean vessel diameter in day 8 infected *Chat*[WT] (black) or T-*Chat*[KO] (white) mice was normalized to the average vessel diameter of naïve mice at each branch depth. Values above 100% (dashed line) indicate increased blood vessel diameter. Mean + SEM, average of n = 2 naïve mice for each genotype used for comparison to values in n = 4 day 8 infected samples in each genotype. Statistical significance determined by unpaired two-tailed t test between day 8 and naïve mice of the same genotype. (**C**) Representative liver arterial tree of T-*Chat*[KO] mice treated with minoxidil or B6 mice treated with L-NAME on days 6 to 8 postinfection. MICROFIL injection was performed on day 8 postinfection with LCMV-Cl13. Scale bars, 2000 μm. (**D**) *Chat*[WT] or T-*Chat*[KO] animals were infected with LCMV-Cl13 and then gavaged with either water (control) or minoxidil hydrochloride dissolved in water daily on days 6 to 12 postinfection. Serum viral titer was determined 30 days postinfection in *Chat*[WT] control (black), *Chat*[WT] minoxidil-treated (blue), T-*Chat*[KO] control (white), or T-*Chat*[KO] minoxidil-treated (yellow) mice. Composite of three to four experimental cohorts, n = 10 to 18.

(**E**) Serum viral titers of C57Bl/6 mice injected with either PBS (black) or L-NAME (green) on days 6 to 12 post–LCMV-Cl13 infection. Composite of three experimental cohorts, n = 10 to 15. (**F**) *Il21r*^{+/+} or *Il21r*^{−/−} animals were infected with LCMV-Cl13 and then gavaged with either water or minoxidil daily on days 6 to 12 postinfection. Serum viral titer was determined 30 days postinfection in *Il21r*^{+/+} control (black), *Il21r*^{+/+} minoxidil-treated (violet), *Il21r*^{−/−} control (white), or *Il21r*^{−/−} minoxidil-treated (red) mice. Each symbol represents an individual mouse, n = 4 to 7. Statistical significance for all samples determined by unpaired two-tailed t test; *P < 0.05, **P < 0.01, ***P < 0.001, ****P < 0.0001.

### REFERENCES AND NOTES

1. M. C. Fishman, *Yale J. Biol. Med.* **45**, 104–118 (1972).
2. O. Loewi, *J. Mt. Sinai Hosp. N. Y.* **24**, 1014–1016 (1957).
3. R. F. Furchgott, J. V. Zawadzki, *Nature* **288**, 373–376 (1980).
4. M. Rosas-Ballina et al., *Science* **334**, 98–101 (2011).
5. C. Reardon et al., *Proc. Natl. Acad. Sci. U.S.A.* **110**, 1410–1415 (2013).
6. P. S. Olofsson et al., *Nat. Biotechnol.* **34**, 1066–1071 (2016).
7. Y. N. Tallini et al., *Physiol. Genomics* **27**, 391–397 (2006).
8. M. A. Cox, S. M. Kahan, A. J. Zajac, *Virology* **435**, 157–169 (2013).
9. A. Fröhlich et al., *Blood* **109**, 2023–2031 (2007).
10. H. Elsaesser, K. Sauer, D. G. Brooks, *Science* **324**, 1569–1572 (2009).
11. A. Fröhlich et al., *Science* **324**, 1576–1580 (2009).
12. J. S. Yi, M. Du, A. J. Zajac, *Science* **324**, 1572–1576 (2009).
13. T. Misgeld et al., *Neuron* **36**, 635–648 (2002).
14. P. P. Lee et al., *Immunity* **15**, 763–774 (2001).
15. J. S. Yi, J. T. Ingram, A. J. Zajac, *J. Immunol.* **185**, 4835–4845 (2010).
16. Y. Tian et al., *J. Immunol.* **196**, 2153–2166 (2016).
17. A. M. Hanash et al., *Blood* **118**, 446–455 (2011).
18. K. G. Anderson et al., *Nat. Protoc.* **9**, 209–222 (2014).
19. H. K. Lee et al., *J. Clin. Invest.* **126**, 2827–2838 (2016).
20. M. P. Doyle, B. R. Duling, *Am. J. Physiol.* **272**, H1364–H1371 (1997).
21. G. Xin et al., *Cell Rep.* **13**, 1118–1124 (2015).
22. S. N. Mueller, L. K. Mackay, *Nat. Rev. Immunol.* **16**, 79–89 (2016).
23. R. S. Herbst et al., *Nature* **515**, 563–567 (2014).
24. C. L. Hsieh et al., *Immunobiology* **216**, 491–496 (2011).
25. S. J. Santegoets et al., *J. Transl. Med.* **11**, 37 (2013).

# Choline acetyltransferase–expressing T cells are required to control chronic viral infection

Maureen A. Cox, Gordon S. Duncan, Gloria H. Y. Lin, Benjamin E. Steinberg, Lisa X. Yu, Dirk Brenner, Luke N. Buckler, Andrew J. Elia, Andrew C. Wakeham, Brian Nieman, Carmen Dominguez-Brauer, Alisha R. Elford, Kyle T. Gill, Shawn P. Kubli, Jillian Haight, Thorsten Berger, Pamela S. Ohashi, Kevin J. Tracey, Peder S. Olofsson, and Tak W. Mak

### ChAT-ty T cells fight viral infection

The neurotransmitter acetylcholine (ACh) is involved in processes such as muscle contraction, neuron communication, and vasodilation. Along with neurons, a population of immunological T cells and B cells express the enzyme choline acetyltransferase (ChAT), which catalyzes the rate-limiting step of ACh production. However, the role of immune cell–derived ACh is unclear. Cox *et al.* report that the cytokine interleukin-21 (IL-21) induces ChAT expression in CD4+ and CD8+ T cells during lymphocytic choriomeningitis virus infection (see the Perspective by Hickman). T cell–specific deletion of ChAT strongly impaired vasodilation and trafficking of antiviral T cells into infected tissues, which undermined the effective control of a chronic viral infection. Thus, IL-21 plays a critical role during chronic infection. Furthermore, the findings reveal a cholinergic mechanism that can regulate immune cell migration into tissues.

*Science*, this issue p. 639; see also p. 585

**View the article online**
https://www.science.org/doi/10.1126/science.aau9072
**Permissions**
https://www.science.org/help/reprints-and-permissions

Use of this article is subject to the Terms of service